DIRAC NOTE 2007–01

Parametrization of $\pi^+\pi^-$ pairs spectra at the DIRAC kinematic range

M. Zhabitsky
JINR Dubna, Russia

January 18, 2007

Abstract

Shape of spectra of $\pi^+\pi^-$ pairs with small relative momentum Q inclusively produced in the reaction $\mathrm{p} + \mathrm{Ni} \to \pi^+\pi^- X$ at 24 GeV/c is presented.

Introduction

The DIRAC analyzes $\pi^+\pi^-$-pairs with small relative momenta Q in their center of mass system in order to find out signal from pionium breakup. One of approaches in analysis does rely on the correct MC simulation of $\pi^+\pi^-$-pairs inclusively produced in pNi-collisions, which are background to pairs from pionium break-up. Physics of pairs and atomic production processes is concentrated in their center of mass system, but, for example, probability of pionium breakup in the target depends on the value of pionium momentum in the target system of reference. Also the adequate transportation of pions through the spectrometer setup and the correct detector response do require the proper description of the pairs spectra shape in the laboratory system.

We will construct acceptance function for $\pi^+\pi^-$ pairs with total momentum $\vec{P}_\Sigma$ and small relative momentum in their center of mass system $\vec{Q}$ as a function of single particle acceptance functions $G^{\pi^-}(\vec{p}_-)$ and $G^{\pi^-}(\vec{p}_+)$. Based on the above pairs acceptance function we will estimate the shape of spectra of $\pi^+\pi^-$ pairs with small Q inclusively produced in the reaction $\mathrm{p} + \mathrm{Ni} \to \pi^+\pi^- X$. The original purpose of this study is a shape suitable for MC simulations. For this reason a simple analytical function which parametrizes the pairs production distribution will be derived. We will analyze leading sources of systematic errors in the shape and later on will compare it to the results of previous studies [1, 2].

1 Acceptance for pairs

We will construct acceptance function for $\pi^+\pi^-$ pairs with total momentum $\vec{P}_\Sigma$ and relative momentum in their center of mass system $\vec{Q}$ as a function of single particle acceptance functions $G^{\pi^-}(\vec{p}_-)$ and $G^{\pi^-}(\vec{p}_+)$:

$$G^{\pi^+\pi^-}(\vec{P}_\Sigma, \vec{Q}) = G^{\pi^+}(\vec{p}_+) G^{\pi^-}(\vec{p}_-) T(\vec{P}_\Sigma, \vec{Q}). \tag{1}$$

Here $\vec{P}_\Sigma$ is a pairs total momentum in the target system of reference (z-axis is along primary proton beam, y-axis is vertical). $\vec{Q}$ is defined in a way, that Q_L is along $\vec{P}_\Sigma$ and Q_x is in xz-plane of secondary particles system of coordinate (see appendix B for details). Single particle acceptance functions $G^{\pi^-}(\vec{p}_-)$ and $G^{\pi^-}(\vec{p}_+)$ were defined in [3].

We will call an MC event reconstructed if following criteria are fulfilled:

- both tracks are reconstructed in DC;
- no signal in N_2 Cherenkov counters;
- no hits in Muon hodoscope;
- hits with proper timing (± 4 ns) in PreShower.

We will introduce space $\Omega^{\pi^+\pi^-}$ where both single particle acceptance functions are high (threshold $G^{\pi^\pm}_{\min}$ is typically set to be about 50% of the maximal acceptance in the $\vec{p}_\pm$ range):

$$\Omega^{\pi^+\pi^-} = \left\{ \vec{p}_+, \vec{p}_- : \quad G^{\pi^\pm}(\vec{p}_\pm) > G^{\pi^\pm}_{\min} \; AND \; |\vec{p}_\pm| \in [1.5, 5.0] \text{ GeV}/c \right\}. \tag{2}$$

Then Ω^Q is some predefined space in pairs center of mass system.

The factor $T(\vec{P}_\Sigma, \vec{Q})$ in the pairs acceptance parametrization (1) can differ from constant either due to detector response (any upstream detector) or due to the trigger system which makes decision based on topology of hits specific to small Q. Below we will show that for analysis of events in certain small Q space with detectors after the spectrometer magnet $T(\vec{P}_\Sigma, \vec{Q})$ is a constant, therefore pairs acceptance function $G^{\pi^+\pi^-}(\vec{P}_\Sigma, \vec{Q})$ is proportional to the product of corresponding single particle acceptance functions.

Most of experimental data collected in 2001-2003 on Ni target was taken with "T1copl×T4×(DNA+RNA)" trigger. "T1 coplanarity" trigger [4] starting from July 2001 used signals from downstream detectors only. Hence it introduces particles correlation only due to co-planarity cut: the difference of hit slab numbers in the horizontal hodoscopes HH(+) and HH(−) of two arms should be $\leqslant 2$. About 2 million of T1 triggers with coplanarity in so-called transparent mode were collected during the dedicated run 6371 (July 2003). Only 1272 of reconstructed in Drift Chambers prompt pairs were in the region with $|Q_x|, |Q_y| < 10$ MeV/c, $|Q_L| < 22$ MeV/c. From fig. 1 one can see that coplanarity cut suppresses pairs with $|Q_y| > 8$ MeV/c.

Other triggers decisions can be checked with "T1-coplanarity" runs which were regularly collected during data-taking. "T4" trigger reconstructs straight tracks in the X-projection of the Drift Chambers and analyzes them with respect to their relative momentum [5]. Its decisions are consistent with track reconstruction algorithm and losses

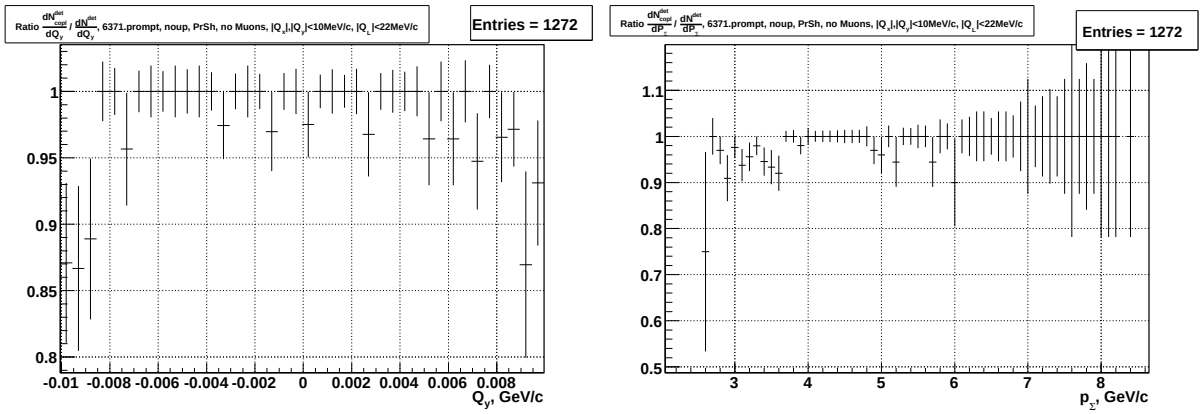

Figure 1: Fraction of positive "coplanarity" decisions as a function of Q_y (left) and P_Σ (right).

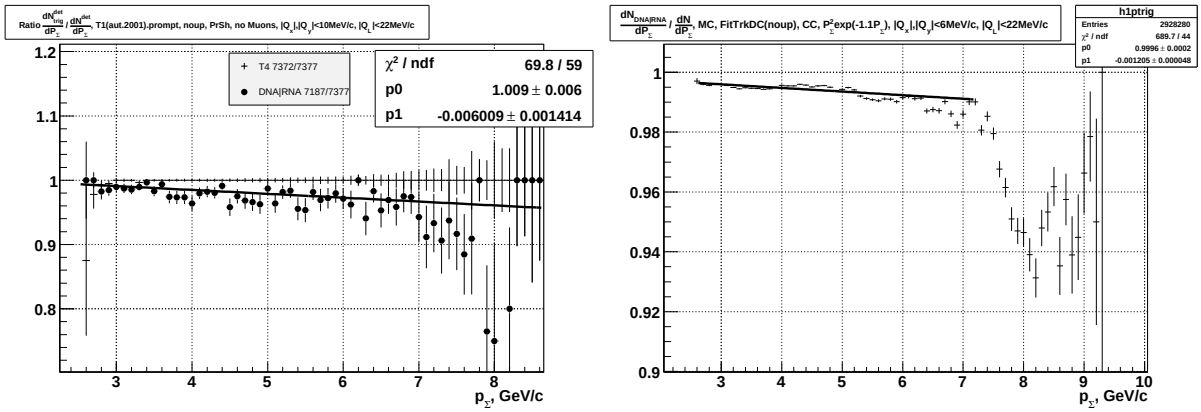

Figure 2: Fraction of positive T4 decisions or positive DNA+RNA decisions as a function of P_Σ in experimental data and in MC simulation.

are negligible (fig. 2). DNA [6] and RNA [5] receive hit patterns from detectors after the magnet, but also use hits from X-planes of the IH (DNA) or the X-plane of the SFD (RNA). Their OR mode shows small bias as a function of pairs total momenta, due to unresolved tracks in presence of background in forward detectors [8]. Despite the experimental bias seems to be qualitatively reproduced in MC simulation [7], we restrict further analysis to experimental runs 3600-3862 which were collected with "T1copl×T4" trigger.

Finally for reconstructed in Drift Chambers pairs with relative momentum in $\Omega^Q = \{|Q_x|, |Q_y| < 8\ \mathrm{MeV}/c,\ |Q_L| < 22\ \mathrm{MeV}/c\}$ (or any subspace of Ω^Q) one can introduce pairs acceptance 2d-function:

$$G^{\pi^+\pi^-}(P_\Sigma, \Theta, \Omega^Q) = \int\limits_{\Omega^{\pi^+\pi^-}\Omega^Q} G^{\pi^+}(\vec{p}_+) G^{\pi^-}(\vec{p}_-) f(\vec{Q}) d^3Q d\varphi. \qquad (3)$$

Here $f(\vec{Q})$ is an (unknown) distribution of pairs on their relative momentum in the center of mass system. This distribution can be obtained from experimental data. It is clear that the shape of experimental distribution on Q is in between uniform distribution (as for Non-Coulomb pairs) and corresponding shape of Coulomb-Correlated pairs. Pairs acceptance function $G^{\pi^+\pi^-}(P_\Sigma, \Theta, \Omega^Q)$ for both Coulomb-Correlated pairs and Non-Coulomb pairs

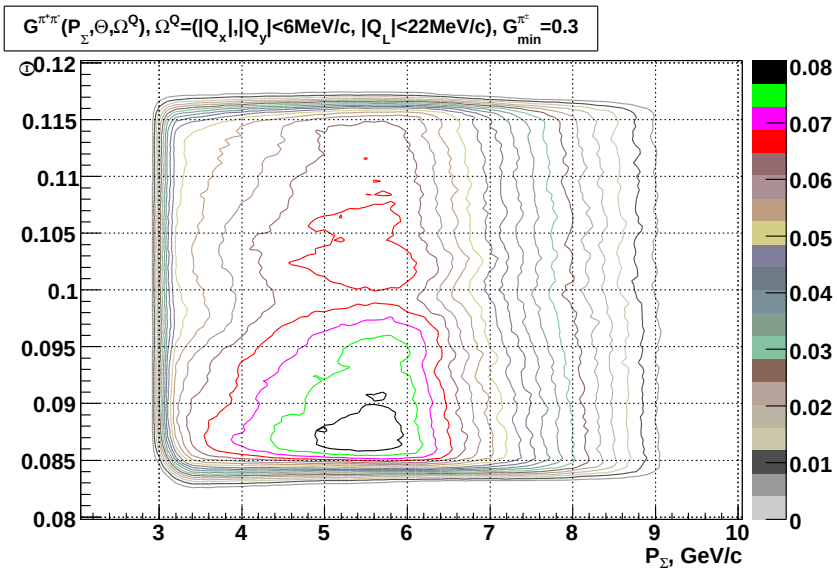

Figure 3: $G^{\pi^+\pi^-}(P_\Sigma, \Theta, \Omega^Q)$ for $\Omega^Q = \{|Q_x|, |Q_y| < 6\ \text{MeV}/c, |Q_L| < 22\ \text{MeV}/c\}$, $G^{\pi^\pm}_{\min} = 0.3$.

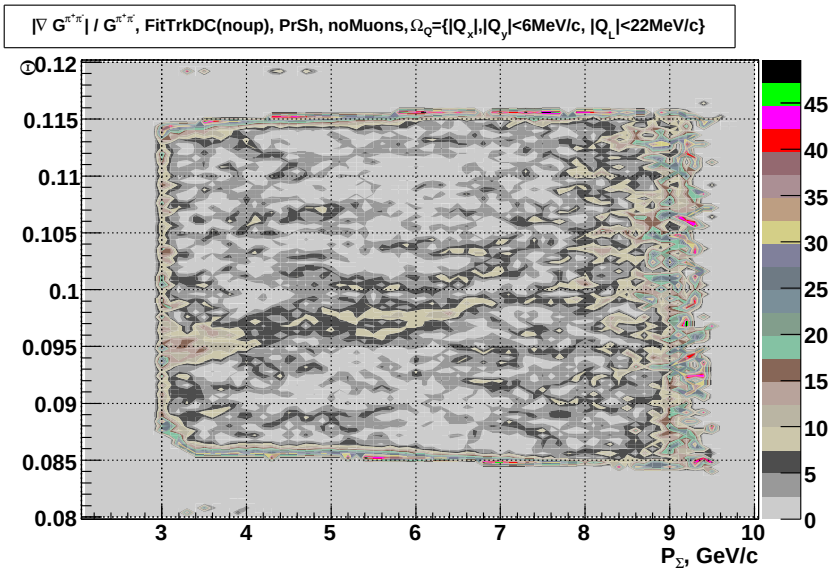

Figure 4: $\dfrac{\nabla G^{\pi^+\pi^-}}{G^{\pi^+\pi^-}(P_\Sigma, \Theta, \Omega^Q)}$ for $\Omega^Q = \{|Q_x|, |Q_y| < 6\,\text{MeV}/c, |Q_L| < 22\,\text{MeV}/c\}$ (regions with $\left|\nabla \ln G^{\pi^+\pi^-}\right| > 50\ [\text{GeV}/c]^{-1}$ have been already removed).

in Ω^Q were found to be very close (their difference has no systematic slopes and is much smaller than uncertainties in the pairs production shape due to different systematic errors). Hereafter we will use Coulomb-Correlated $f(\vec{Q})$, as Coulomb-Correlated pairs are most of pairs of interest.

Typical $G^{\pi^+\pi^-}(P_\Sigma, \Theta, \Omega^Q)$ distribution is shown in fig. 3. This distribution is used to define the region of fitting, which is the (P_Σ, Θ) area where $\left|\nabla \ln G^{\pi^+\pi^-}\right| < 20\ [\text{GeV}/c]^{-1}$ (fig. 4). This criteria eliminates regions which are close to acceptance edges.

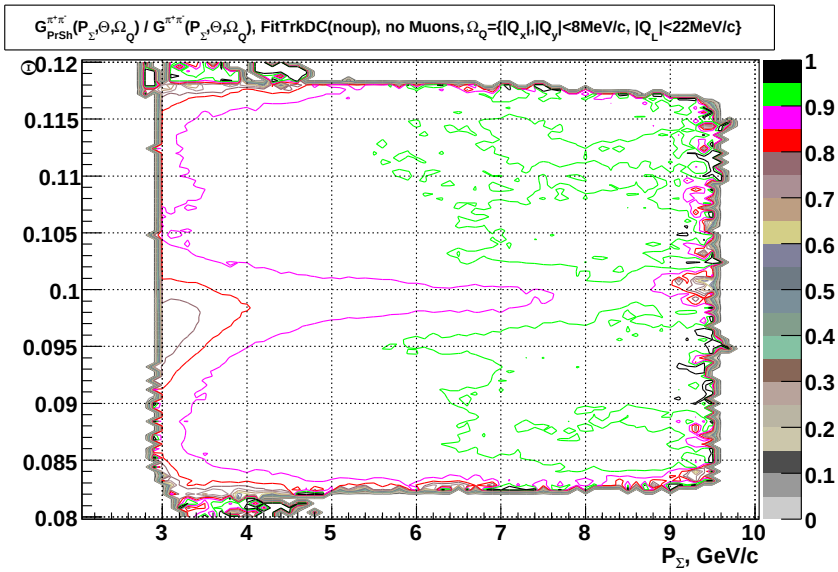

Figure 5: Estimated fraction of events when both tracks have proper time signals in PrSh as a function of P_Σ and Θ for MC CC pairs with $|Q_x|, |Q_y| < 8\,\mathrm{MeV}/c, |Q_L| < 22\,\mathrm{MeV}/c$.

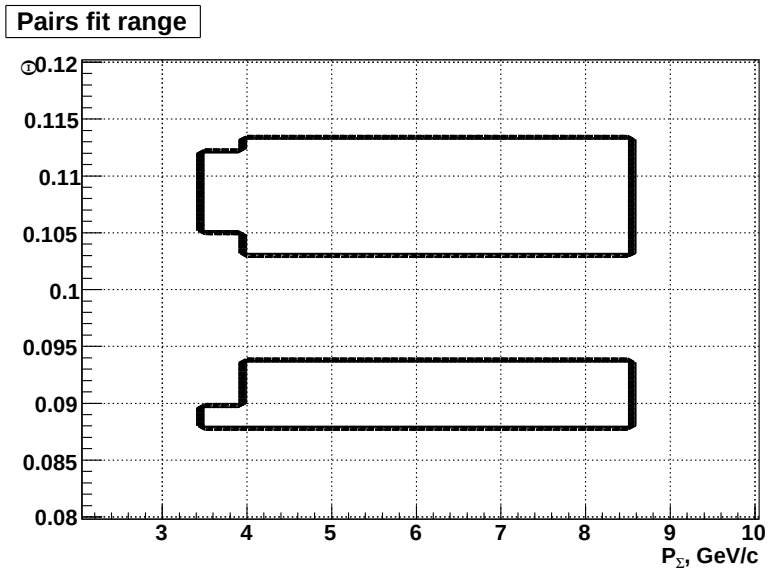

Figure 6: (P_Σ, Θ) area, where fitting will be performed.

In fig. 3 one can see event suppression around $\Theta = 0.1$ due to interaction of pions with the Al frame of Cherenkov detector. Losses are clearly seen if one analyzes MC data with and without PrSh hit requirement (fig. 5). Unfortunately, PrSh signals are required for T1 trigger. Moreover the experimental losses due to this effect are not reproduced quantitatively in MC, so events with Θ around 0.1 have to be removed from analysis. For single particle acceptance functions $G^{\pi^\pm}$ this dip is for $\Theta_\pm \in [0.095, 0.102]$. Then for pairs acceptance function the suppression is in the range $\Theta_\Sigma \in [0.093, 0.104]$ if one uses $|Q_x|, |Q_y| < 6\,\mathrm{MeV}/c$ cut. If cut is $|Q_x|, |Q_y| < 8\,\mathrm{MeV}/c$ then dip is extended to $\Theta_\Sigma \in [0.092, 0.105]$. Moreover, PrSh efficiency in MC decreases for low P_Σ.

Finally, the simplified (P_Σ, Θ) area, where fitting will be performed, is shown in fig. 6.

2 Experimental data

Experimental data collected with "T1pipicoplanarity×T4" trigger on Ni 94 μm target in 2001 (3600–3862 runs) was analyzed. Selected events fulfill following criteria:

- tracks in positive and negative arms are reconstructed in DC (only 1×1 combinations), advanced tracking (FitTrkDC) is used;
- no signals in N_2 Cherenkov counters;
- no hits in Muon hodoscope;
- hits with proper timing (± 4 ns) in PreShower;
- both particles are in regions with well defined acceptance (pair is inside $\Omega^{\pi^+\pi^-}$);
- reconstructed pair relative momentum Q in its CMS is within predefined Ω_Q.

We will define detected double differential distribution as

$$\frac{d^2N^{\rm det}}{dP_\Sigma d\Theta} = \int\limits_{\Omega^{\pi^+\pi^-}\Omega^Q} \frac{d^6N^{\rm det}}{d^3P_\Sigma d^3Q} d^3Q d\varphi. \tag{4}$$

Then production distribution of $\pi^+\pi^-$ pairs inclusively produced in pNi-collisions can be estimated after subtraction of so-called background of accidentals:

$$\frac{d^2N}{dP_\Sigma d\Theta} = \frac{1}{G^{\pi^+\pi^-}(P_\Sigma,\Theta,\Omega^Q)} \left(\frac{d^2N^{\rm det}_{\Delta t=[-0.5,0.5]\rm ns}}{dP_\Sigma d\Theta} - c\frac{d^2N^{\rm det}_{\Delta t=[-12,-5]\rm ns}}{dP_\Sigma d\Theta} \right). \tag{5}$$

Production distribution $\dfrac{d^2N}{dP_\Sigma d\Theta}$ ("distribution on target") was fitted by Badhwar parametrization of LIDCS (see Appendix A for details) in the region shown in fig. 6. For $\Omega_Q = \{|Q_x|, |Q_y| < 6\,\mathrm{MeV}/c, |Q_L| < 22\,\mathrm{MeV}/c\}$ slices of the pairs production distribution with superimposed fits are shown for fixed values of Θ (fig. 7) and fixed values of total momenta P_Σ (fig. 8). Fit parameters are presented in table 1. In the DIRAC acceptance pairs transverse momentum $P_\perp \in [0.25, 0.9]$ GeV/c. For the most part of data $P_\perp$ is less than 0.5 GeV/c, therefore C_2 and C_3 parameters works as corrections for the leading term in the Badhwar parametrization. Moreover fit with $C_2 = C_3 = 0$ provides χ^2/NDF close

Table 1: Fit parameters for pairs production (method "G")

Ω_Q	$N_{\rm events}$*	B	C_1	χ^2/NDF
$\lvert Q_x\rvert, \lvert Q_y\rvert < 4\,\mathrm{MeV}/c, \lvert Q_L\rvert < 22\,\mathrm{MeV}/c$	95228	4.03 ± 0.11	8.47 ± 0.18	3363/1998
$\lvert Q_x\rvert, \lvert Q_y\rvert < 6\,\mathrm{MeV}/c, \lvert Q_L\rvert < 22\,\mathrm{MeV}/c$	203765	4.03 ± 0.07	7.47 ± 0.11	2452/1998
$\lvert Q_x\rvert, \lvert Q_y\rvert < 8\,\mathrm{MeV}/c, \lvert Q_L\rvert < 22\,\mathrm{MeV}/c$	346334	3.98 ± 0.05	7.44 ± 0.08	2710/1998
$Q < 6\,\mathrm{MeV}/c$	39454	4.07 ± 0.16	10.3 ± 0.26	4012/1970
$Q < 8\,\mathrm{MeV}/c$	83533	3.68 ± 0.11	8.85 ± 0.17	3119/1996

* $N_{\rm events}$ — number of selected events in the region of fitting

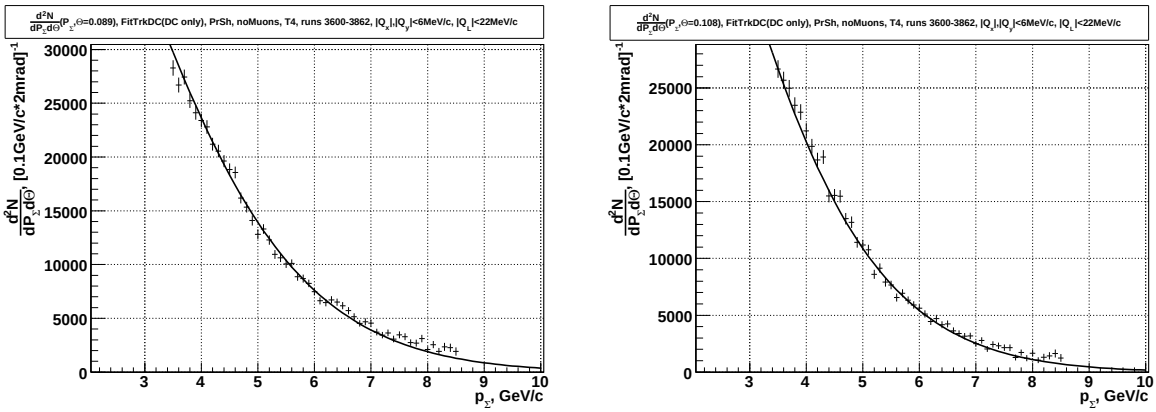

Figure 7: $\dfrac{d^2N}{dP_\Sigma d\Theta}\left(p + \mathrm{Ni} \to \pi^+\pi^- X\right)$ for fixed values of pairs polar angle Θ: 0.089 (left), 0.108 (right).

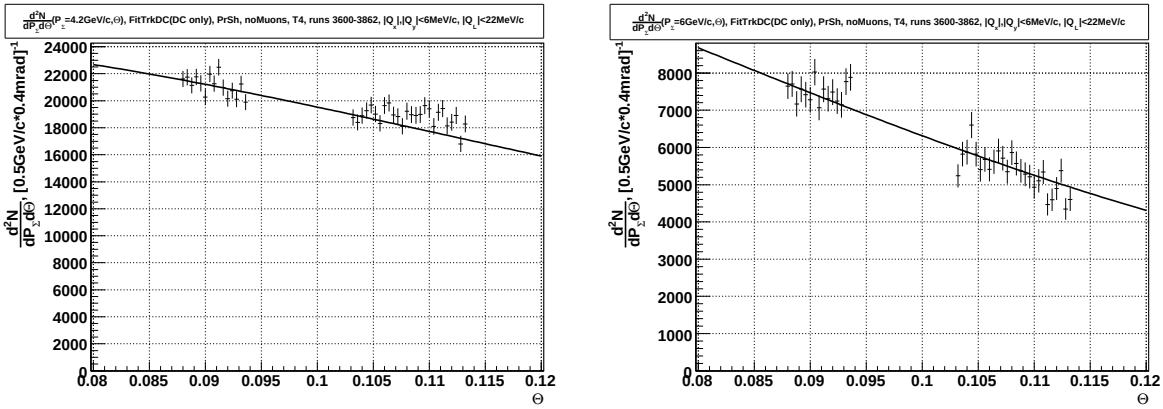

Figure 8: $\dfrac{d^2N}{dP_\Sigma d\Theta}\left(p + \mathrm{Ni} \to \pi^+\pi^- X\right)$ for fixed values of pairs total momenta P_Σ: 4.2 GeV/c (left), 6 GeV/c (right).

to the corresponding ratio for the fit with C_2 and C_3 as free parameters. Hereafter we will present only fit results with fixed values of $C_2 = C_3 = 0$.

Volume $\Omega_Q = \{|Q_x|, |Q_y| < 6\ \mathrm{MeV}/c, |Q_L| < 22\ \mathrm{MeV}/c\}$ corresponds to about 2σ resolution on transversal components of pairs relative momentum in their center-of-mass system. Distributions and fit parameters for this volume are chosen as reference. Fits for other Ω_Q provide similar results, but samples with more restrictive cuts on $|Q_x|, |Q_y|$ or spherically-symmetrical cut on Q contain less data. From the outer side available volume Ω_Q is limited by the trigger cuts. Clearly seen in figure 10 slope[1] in ratios of different parametrizations from table 1 is less than 0.05 $[\mathrm{GeV}/c]^{-1}$. It has to be emphasized that selection of events from different Ω_Q does not produce any slope in momentum distributions (based on available statistics) neither for detected events nor for detected events corrected according to acceptance (fig. 9). Therefore slope in the ratio of parametrizations has to be attributed to uncertainties due to the over simplified analytic function chosen for fitting (this is also clear from χ^2/NDF values from table 1).

[1]Hereafter we will measure slope as a value of α in the linear expansion $c(1 + \alpha P_\Sigma)$.

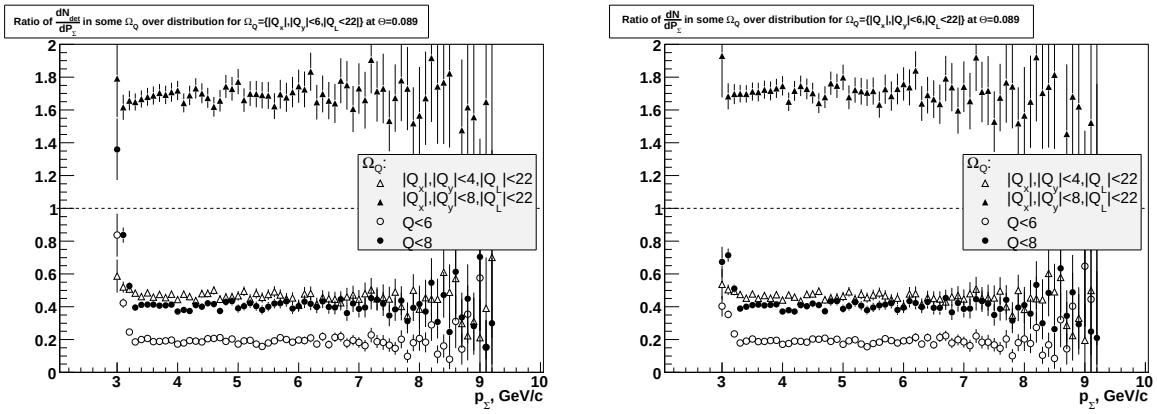

Figure 9: Ratios of $\dfrac{d^2N^{\rm det}}{dP_\Sigma d\Theta}$ (left) and $\dfrac{d^2N}{dP_\Sigma d\Theta}$ (right) of $\pi^+\pi^-$ pairs from different Ω_Q over corresponding distributions of pairs from $\Omega_Q = \{|Q_x|, |Q_y| < 6\,\mathrm{MeV}/c, |Q_L| < 22\,\mathrm{MeV}/c\}$ at fixed polar angle $\Theta = 0.089$.

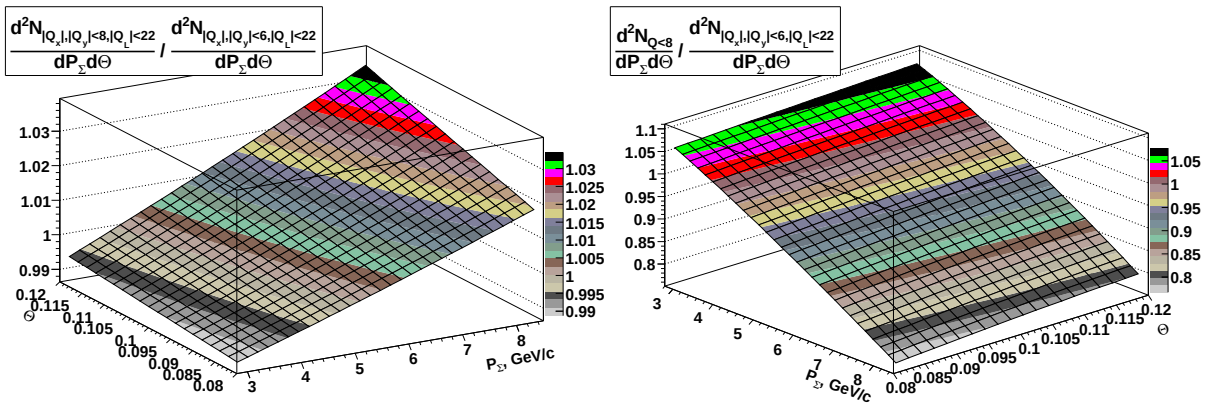

Figure 10: Ratios of production parametrizations (Table 1) for $\pi^+\pi^-$ pairs with $|Q_x|, |Q_y| < 8\,\mathrm{MeV}/c, |Q_L| < 22\,\mathrm{MeV}/c$ (left) and $Q < 8\,\mathrm{MeV}/c$ (right) over the reference parametrization of pairs from $\Omega_Q = \{|Q_x|, |Q_y| < 6\mathrm{MeV}/c, |Q_L| < 22\mathrm{MeV}/c\}$. Production distributions are normalized to provide the same integral.

Alternatively, pairs production double differential cross-section can be obtained by the iterative method:

$$\frac{d^2N^i_{\rm MC}}{dP_\Sigma d\Theta} = \frac{d^2N^{i-1}_{\rm MC}}{dP_\Sigma d\Theta} \frac{\dfrac{d^2N^{\rm det}_I}{dP_\Sigma d\Theta}}{\dfrac{d^2N^{i-1\,{\rm det}}_{\rm MC}}{dP_\Sigma d\Theta}}. \tag{6}$$

Here "detected" distributions are defined as

$$\frac{d^2N^{\rm det}_I}{dP_\Sigma d\Theta} = \int_0^{2\pi}\int_{\Omega^Q} \frac{d^6N^{\rm det}}{d^3P_\Sigma d^3Q} d^3Q d\varphi \tag{7}$$

(compare to (4) where data is taken only from regions with the well defined acceptance). The simple shape

$$\frac{d^2N^0_{\rm MC}}{dP_\Sigma d\Theta} \propto P_\Sigma^2 \exp(-1.1P_\Sigma) \tag{8}$$

was used as the initial condition and the only one step in iteration was done. Generated MC sample was approximately 5 times larger than the experimental one. Resulting distribution $\dfrac{d^2N^1_{\rm MC}}{dP_\Sigma d\Theta}$ was fitted by the Badhwar function in the same region as for the previous method and fit parameters are presented in the table 2. Results of both methods are consistent (see fig. 11, right). Distribution based on simple shape (8) seems to be a reasonable approximation for MC generation with appropriate weights applied during next stages of analysis (fig. 11, left).

Table 2: Fit parameters for pairs production (iterative method "I"); $\Omega_Q = \{|Q_x|, |Q_y| < 6\ {\rm MeV}/c, |Q_L| < 22\ {\rm MeV}/c\}$.

	$N_{\rm events}$	B	C_1	χ^2/NDF
DC only	210633	4.09 ± 0.07	7.18 ± 0.12	2147/1998

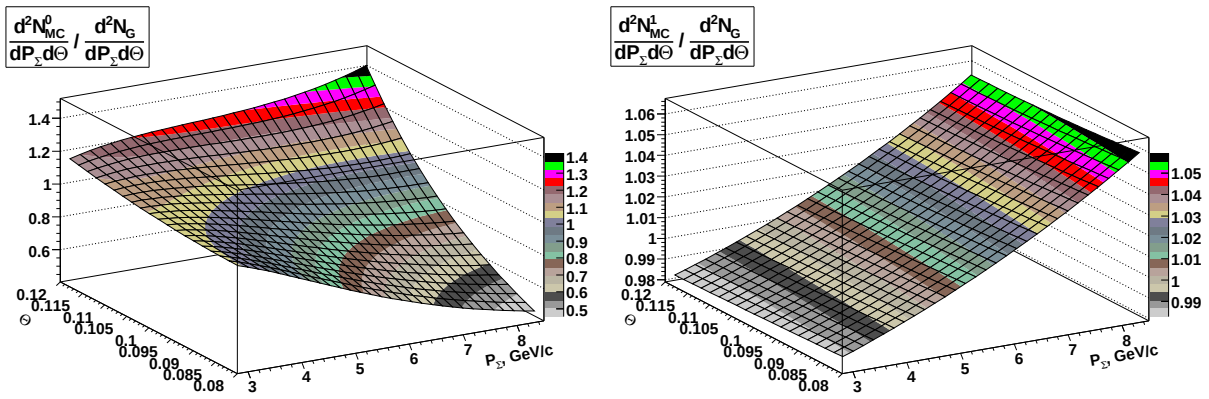

Figure 11: $\dfrac{d^2N^0_{\rm MC}}{dP_\Sigma d\Theta}\Big/\dfrac{d^2N_G}{dP_\Sigma d\Theta}$ (left) and $\dfrac{d^2N^1_{\rm MC}}{dP_\Sigma d\Theta}\Big/\dfrac{d^2N_G}{dP_\Sigma d\Theta}$ (right) for p + Ni $\to \pi^+\pi^-X$ in the DIRAC kinematic range ($\Omega_Q = \{|Q_x|, |Q_y| < 6\ {\rm MeV}/c, |Q_L| < 22\ {\rm MeV}/c\}$). Production distributions are normalized to provide the same integral.

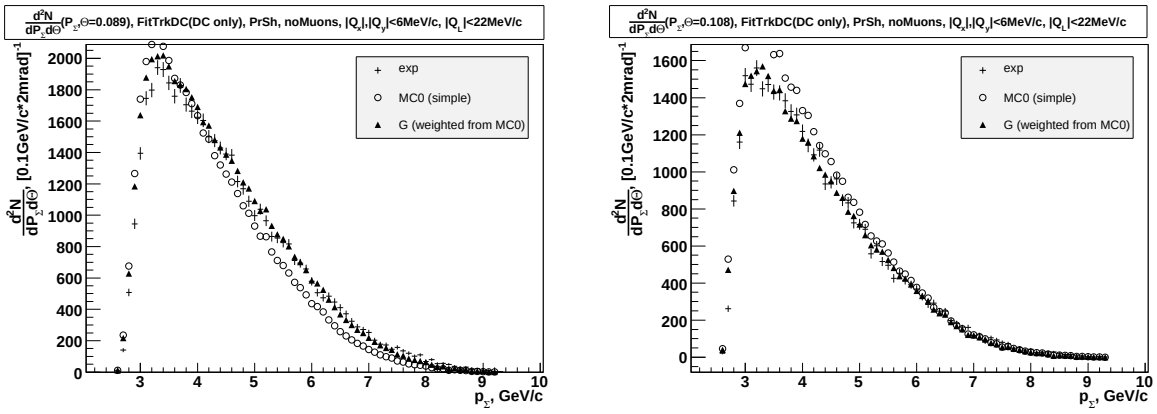

Figure 12: $\dfrac{d^2N_I^{\rm det}}{dP_\Sigma d\Theta}\left(p+{\rm Ni}\to\pi^+\pi^-X\right)$ for fixed values of pairs polar angle Θ: 0.089 (left), 0.108 (right).

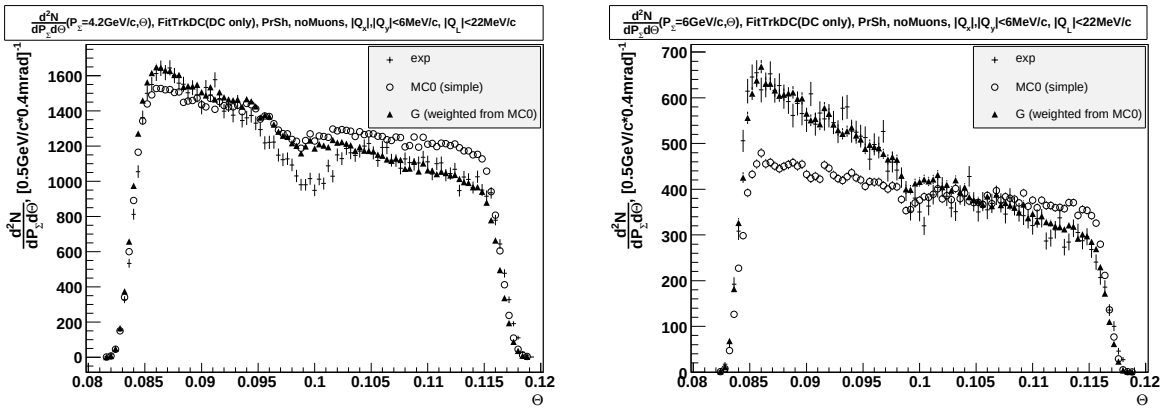

Figure 13: $\dfrac{d^2N_I^{\rm det}}{dP_\Sigma d\Theta}\left(p+{\rm Ni}\to\pi^+\pi^-X\right)$ for fixed values of pairs total momenta P_Σ: 4.2 GeV/c (left), 6 GeV/c (right).

For cross-check one can compare generated MC distributions to detected experimental distributions for fixed values of Θ (fig. 12) and for fixed values of total momenta P_Σ (fig. 13). Only MC distributions based on the simple formula (MC0) and corresponding distributions from method "G" are shown (distributions for iterative method "I" are indistinguishable from distributions from method "G" at this scale).

2.1 Comparison to the previous results

Double differential pair production shapes from table 1 can be compared to distributions used by *DIRAC event generator* [2]. This generator provides the pairs production shape as a 2D-histogram. Unfortunately, only bin contents, but not bin errors, are known (later on we attach to each bin $\sqrt{\text{bin content}}$ error bars, which seems to be an overestimation). Ratio of this 2D-histogram over the parametrization $\dfrac{d^2N_G}{dP_\Sigma d\Theta}$ is shown in fig. 14. Average relative slope in the ratio is about -0.04 $[\text{GeV}/c]^{-1}$. It has to be noticed that the above 2D-histogram provides reasonable shape only in the "inner" part of acceptance. Closer to acceptance edges its shape starts to diverge.

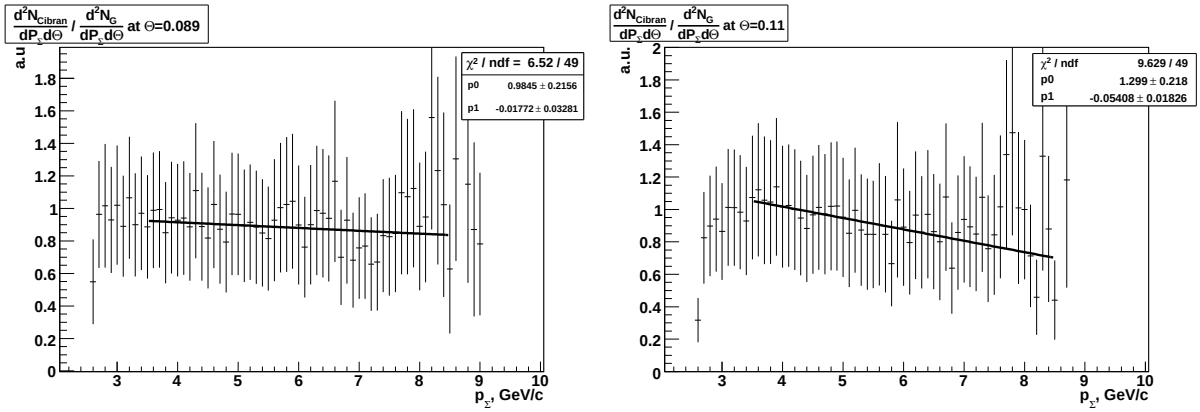

Figure 14: $\dfrac{d^2N_{\text{Cibran}}}{dP_\Sigma d\Theta} \Big/ \dfrac{d^2N_G}{dP_\Sigma d\Theta}$ for $p + \text{Ni} \to \pi^+\pi^- X$ at different pairs polar angles Θ: 0.089 (left) and 0.11 (right). Ratios are fitted by $p0 \cdot (1 + p1 \cdot P_\Sigma)$.

2.2 PrSh in trigger

All statistics was collected with PrSh in T1 trigger, except two runs 4630–4631 in June 2002 when PrSh was out of the trigger. Overall number of collected events in two runs is about 1M, only 5791 of them are $\pi^+\pi^-$ pairs reconstructed in DC with $|Q_x|, |Q_y| < 8\,\text{MeV}/c$, $|Q_L| < 22\,\text{MeV}/c$ and negative "Muon" marks. Without surprise distribution of these events on pairs polar angle has no dip around $\Theta = 0.1$ (fig. 15).

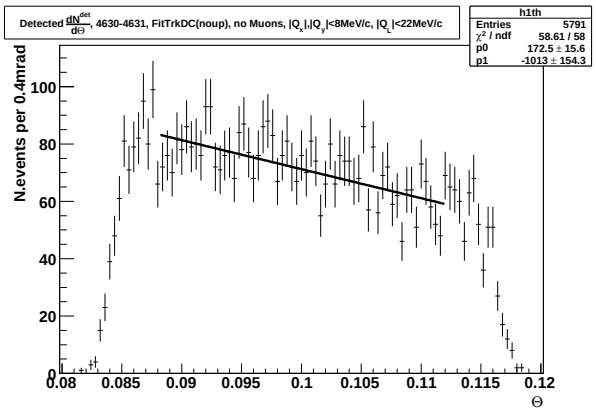

Figure 15: $\dfrac{dN^{\text{det}}}{d\Theta}$ for $\pi^+\pi^-$ pairs with $|Q_x|, |Q_y| < 8\,\text{MeV}/c$, $|Q_L| < 22\,\text{MeV}/c$ from runs 4630–4631.

To estimate bias due to PrSh in pairs spectra, we will first estimate slope in "on target" spectra of accidental π^- (formula (5) from [3]):

$$\frac{d^2N}{dpd\Theta} = \frac{1}{\int\limits_{\Omega^{\pi^-}} G^{\pi^-}(p,\Theta,\varphi)d\varphi} \int\limits_{\Omega^{\pi^-}} \frac{d^3N^{\rm det}}{dpd\Theta d\varphi} d\varphi. \tag{9}$$

Then we will define $f_{\rm noPrSh} = \dfrac{d^2N}{dpd\Theta}$ based on data from runs 4630–4631 and without PrSh requirements in experimental data and in G^{π^-} definition; $f_{\rm PrSh}$ will stand for the "standard" double differential distribution based on data from T4 runs 4621–4648 (with PrSh in T1 trigger), signals from PrSh are required in both experimental data and G^{π^-} definition. Ratio $f_{\rm noPrSh}/f_{\rm PrSh}$ is shown in fig. 16 as a function of pion momenta. For $\Theta \in [0.085, 0.095]$ it can be approximated by a linear function, while for $\Theta \in [0.105, 0.115]$ it has structure more complex than linear. Relative slope in the ratio is $-(0.03 \div 0.04)$ $[\mathrm{GeV}/c]^{-1}$. The similar slope is expected in the positive arm. Finally slope in the small Q pairs production spectra as a function of pairs total momenta is about the average of slopes in negative and positive arms, estimated to be about $-(0.03 \div 0.04)$ $[\mathrm{GeV}/c]^{-1}$.

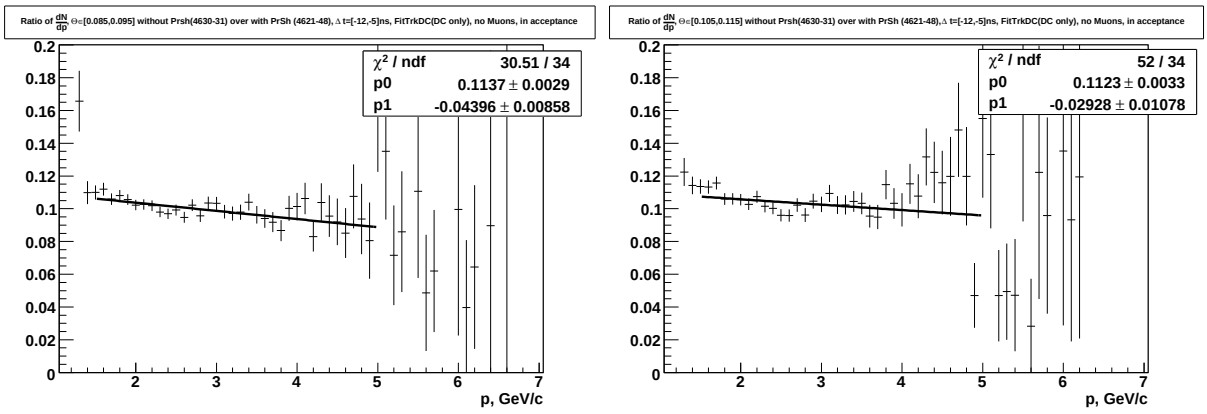

Figure 16: Ratio of $\dfrac{d^2N}{dpd\Theta}$ for accidental π^- from runs without PrSh (4630–4631) over corresponding distribution from runs with PrSh (4621–4648) for $\Theta \in [0.085, 0.095]$ (left) and for $\Theta \in [0.105, 0.115]$ (right). Both ratios are fitted by $p0 \cdot (1 + p1 \cdot p)$.

During runs 4630–4631 percentage of events reconstructed in DC [9] dropped to about 70% with respect to the number of collected $\pi\pi$ triggers. With PrSh in trigger this percentage was about 77%. Difference between these two numbers estimates number of triggered non-target events suppressed thanks to the PrSh to be within 10%, which is not a challenge for trigger/DAQ systems. These non-target events are anyway suppressed by the track reconstruction procedure. Introduction of PrSh signals to the trigger decreases overall detection efficiency (e.g. estimated as the ratio of good "Ntuple-selected" events to the proton flux [9, 10]) by 15%. At the moment data from the PrSh combined with N_2 Cherenkov signals is used only for the estimation of e^+e^- background. Proper PrSh TDC hits are not required by event-by-event analysis [8], even though PrSh is in T1 trigger. Check for presence of positive PrSh signals would suppress additional 10–15% of events.

2.3 Experimental spectra for 20/24 GeV/c

Part of DIRAC statistics was collected with proton beam momenta 20 GeV/c. Center-of-mass energy $\sqrt{s}$ in proton-nucleon collisions is lower by about 10%: from 6.84 GeV at 24 GeV/c to 6.27 GeV at 20 GeV/c. Strangely the ratio of detected distributions of pairs with small Q on total momenta P_Σ at different proton beam momenta (fig. 17) doesn't show expected suppression of pairs with high P_Σ at 20 GeV/c proton beam momenta (fig. 18). Observed relative slope $\alpha = -0.02\,[\mathrm{GeV}/c]^{-1}$ is smaller than the predicted slope of $-0.07\,[\mathrm{GeV}/c]^{-1}$, though suppression can be hidden due to systematic uncertainties. This effect is similar to the discrepancy in shapes of inclusive π^- distributions [3].

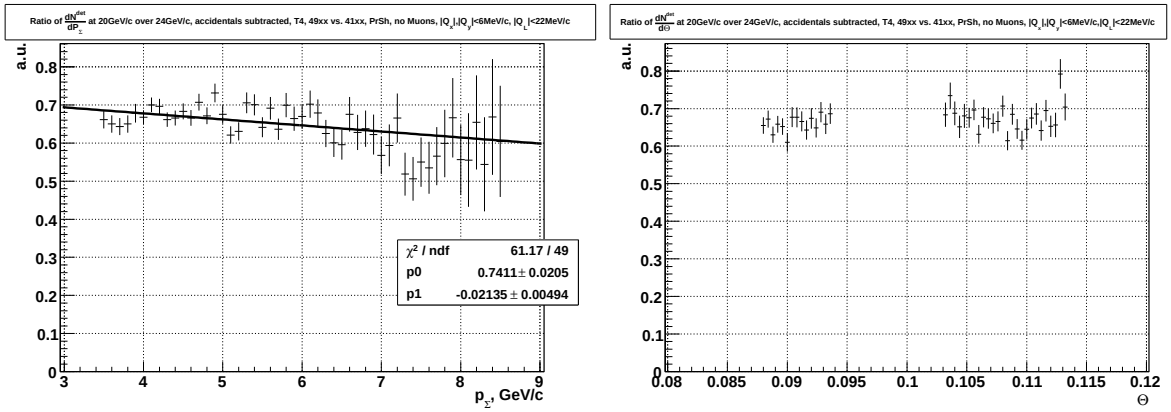

Figure 17: Ratio of detected distributions of pairs with small Q at different proton beam momenta (20 GeV/c over 24 GeV/c) as a function of pairs total momenta P_Σ and polar angle Θ.

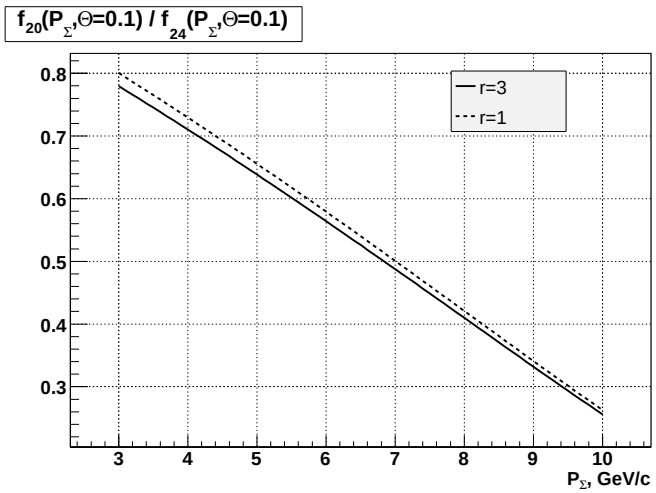

Figure 18: Ratio of Badhwar parametrizations of small Q $\pi^+\pi^-$ pairs inclusive production at incident proton momenta 20 GeV/c over 24 GeV/c as a function of pairs total momenta P_Σ.

3 $P_{\rm br}$ as a function of pairs spectra shape

It was shown that shapes of atomic, Coulomb-correlated (CC) and non-Coulomb (NC) pairs as a function of their CMS relative momentum Q (or Q_L) are nearly not sensitive to the distribution of pairs on total momenta (they could due to multiple scattering and resolution/efficiency dependence on momentum). But as L. Tauscher suggested breakup probability $P_{\rm br}$ as a function of the $\pi^+\pi^-$ atom lifetime τ can vary due to the strong dependence of $P_{\rm br}$ on values of pairs total momentum P_Σ (fig. 19). On the pictures below upper limit for $P_{\rm br}$ is shown. Upper limit corresponds to $P_{\rm br}$ calculation when all atoms excited to level with principal quantum number $n > n_{\max}$ are supposed to be ionized. For calculations $n_{\max} = 8$ was used.

In figure 20 experimental distribution of pairs with small Q (with accidentals subtracted) is split between Coulomb-correlated (CC) and non-Coulomb (NC) pairs by the approximation of the $w_l(P_\Sigma)$ function from FRITIOF-6:

$$w_l(P_\Sigma) = \frac{dN_{\rm NC}}{dP_\Sigma} \Big/ \left(\frac{dN_{\rm CC}}{dP_\Sigma} + \frac{dN_{\rm NC}}{dP_\Sigma} \right) = \exp(-0.4066 - 0.2864 \cdot P_\Sigma), \quad P_\Sigma \text{ is in GeV}/c. \quad (10)$$

$$P_{\rm br}(\tau) = \int_{3.0}^{8.4} P_{\rm br}\left(\tau, P_\Sigma\right) \frac{dN}{dP_\Sigma} dP_\Sigma \Big/ \int_{3.0}^{8.4} \frac{dN}{dP_\Sigma} dP_\Sigma. \quad (11)$$

From kinematics non-Coulomb pairs are expected to have softer spectra. As $P_{\rm br}(P_\Sigma)$ is a monotonously rising function of P_Σ (see fig. 19), if one supposes distribution on P_Σ of CC pairs to have the same shape as for NC pairs, this pushes $P_{\rm br}(\tau)$ downward by $\approx 0.7\%$, as shown in fig. 21(left) by the dashed line. So far this shift is small but shape of $w_l(P_\Sigma)$ has to be proved (measured) in some way.

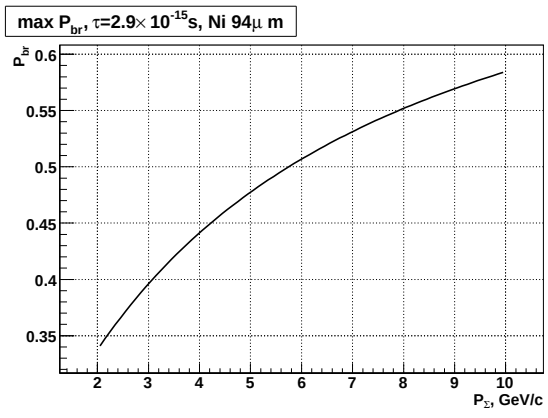

Figure 19: Upper limit for $P_{\rm br}$ as a function of pionium momentum P_Σ for $\tau = 2.9 \cdot 10^{-15}$ s.

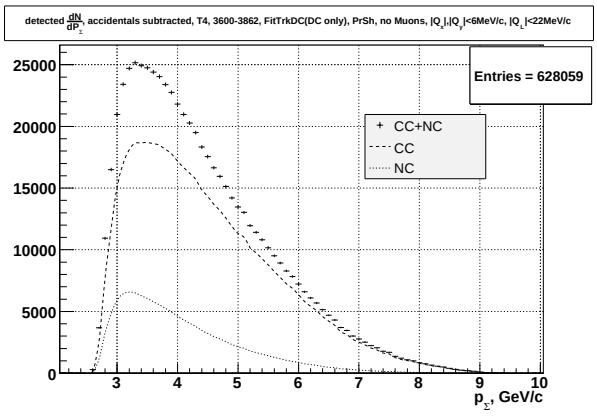

Figure 20: Experimental distribution of pion pairs with small Q from p + Ni $\rightarrow$ $\pi^+\pi^- X$ detected by DIRAC setup. CC and NC components are split according to formula (10).

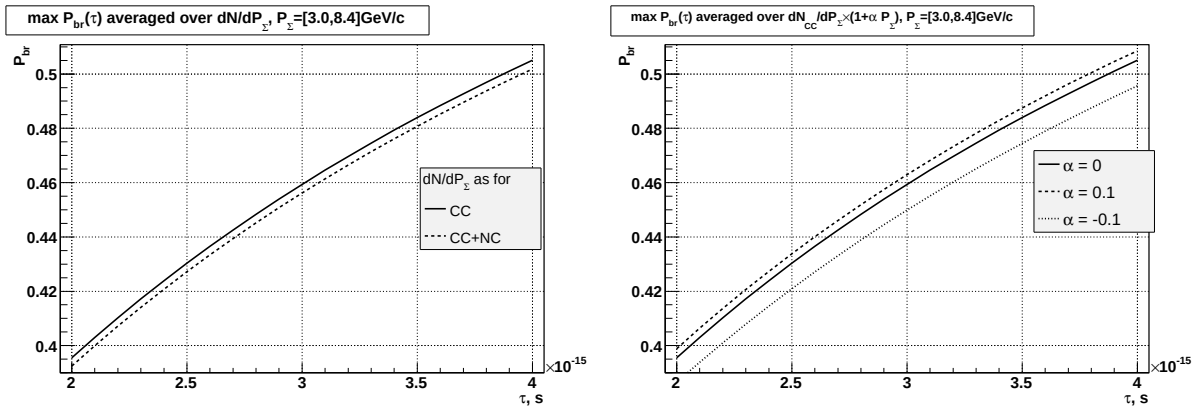

Figure 21: Upper limit for $P_{\rm br}(\tau)$ averaged over distribution on P_Σ:
left — spectra of CC pairs (solid line) and of all pairs (dashed line);
right — spectra of CC pairs modified by $(1 + \alpha P_\Sigma)$ multiplier.

Sensitivity of $P_{\rm br}(\tau)$ to the shape of pairs spectra was estimated by modification of dN_{CC}/dP_Σ by a linear multiplier $(1 + \alpha P_\Sigma)$ (fig. 21(right)). Resulting sensitivity of $P_{\rm br}$ to the value of slope α is presented in Table 3.

Table 3: Sensitivity of $P_{\rm br}(\tau)$ to the shape of pairs spectra

$\alpha, [\mathrm{GeV}/c]^{-1}$	$\Delta P_{\rm br}/\, P_{\rm br}$
0.1	0.78%
0.05	0.46%
−0.05	−0.74%
−0.1	−2.09%

Conclusions

We constructed acceptance function for $\pi^+\pi^-$ pairs with total momentum $\vec{P}_\Sigma$ and small relative momentum in their center of mass system $\vec{Q}$ as a product of single particle acceptance functions $G^{\pi^-}(\vec{p}_-)$ and $G^{\pi^-}(\vec{p}_+)$. It was proved that the above parametrization is valid for $\pi^+\pi^-$ pairs with $|Q_x|, |Q_y| < 8\,\mathrm{MeV}/c$ and $|Q_L| < 22\,\mathrm{MeV}/c$ reconstructed by detectors after the spectrometer magnet.

Based on the above pairs acceptance function we estimated the shape of spectra of $\pi^+\pi^-$ pairs with small Q inclusively produced in the reaction $\mathrm{p}+\mathrm{Ni} \to \pi^+\pi^- X$. The pairs production shape was parametrized by a simple analytical function, which covers the full kinematic region of DIRAC and is suitable for MC simulations.

Major sources of systematic errors were analyzed. Leading error is due to the presence of PrSh signals in T1 trigger, which distorts spectra and also reduces quality and statistics of collected $\pi^+\pi^-$ pairs. It is recommended to exclude PrSh signals from the trigger system during next data runs.

A Spectra parametrization

To fit pairs spectra we adjust parametrization of LIDCS[2] for $p + p \to \pi^- X$ suggested by Badhwar et al. [11]:

$$E\frac{d^3\sigma}{d^3P_\Sigma} = A_{\mathrm{cs}}\frac{(1-\tilde{x})^q}{(1+4m_p^2/s)^3}\exp\left[-BP_\perp/(1+4m_p^2/s)\right], \tag{12}$$

$$\tilde{x} = \frac{E^*}{E^*_{\max}} \simeq \sqrt{x_\parallel^{*2} + \frac{4}{s}(P_\perp^2 + M^2)}, \quad x_\parallel^* = \frac{P_\parallel^*}{P^*_{\max}}, \tag{13}$$

$$q = \frac{C_1 + C_2P_\perp + C_3P_\perp^2}{\sqrt{1+4m_p^2/s}}. \tag{14}$$

Here $M = 2m_\pi\sqrt{1+\left(\frac{Q}{2m_\pi}\right)^2}$ is a pairs effective mass. Inside volume $\Omega^Q = \{|Q_x|, |Q_y| < 6\ \mathrm{MeV}/c, |Q_L| < 22\ \mathrm{MeV}/c\}$ $\dfrac{M}{2m_\pi} < 1.004$, therefore $M \approx 2m_\pi$ is a reasonable approximation. Constants A_{cs}, B, C_1, C_2, C_3 are free parameters.

Double differential production cross section $\dfrac{d^2\sigma}{dpd\Theta}$ can be expressed as

$$\frac{d^2\sigma}{dpd\Theta} = \frac{2\pi p^2\sin\Theta}{E}\left(E\frac{d^3\sigma}{d^3p}\right)\Bigg|_{\mathrm{Badhwar}}. \tag{15}$$

[2]LIDCS — Lorentz invariant differential cross section

B $\vec{Q}$ components as used by DIRAC

Let $\vec{P}_\Sigma = \vec{p}_+ + \vec{p}_- = \{P_x, P_y, P_z\}$ be in the secondary horizontal system of reference $\{\vec{e}_x, \vec{e}_y, \vec{e}_z\}$[3]. Then $\vec{v'} = \{v'_x, v'_y, v'_z\}$ — vector components in a new system of reference $\{\vec{e'_x}, \vec{e'_y}, \vec{e'_z}\}$, which fulfills following conditions:

1. $\vec{e'_z} \uparrow\uparrow \vec{P}_\Sigma$,
2. $\vec{e'_x}$ is in the plane $\{\vec{e}_x, \vec{e}_z\}$.

It is straightforward to express $\{\vec{e'_x}, \vec{e'_y}, \vec{e'_z}\}$ through $\{\vec{e}_x, \vec{e}_y, \vec{e}_z\}$:

$$\begin{aligned}
\vec{e'_x} &= \frac{(P_z\vec{e}_x - P_x\vec{e}_z)}{\sqrt{P_x^2 + P_z^2}}, \\
\vec{e'_y} &= \frac{-P_xP_y\vec{e}_x + (P_x^2 + P_z^2)\,\vec{e}_y - P_yP_z\vec{e}_z}{|\vec{P}_\Sigma|\sqrt{P_x^2 + P_z^2}}, \\
\vec{e'_z} &= \frac{\vec{P}_\Sigma}{|\vec{P}_\Sigma|} = \frac{1}{|\vec{P}_\Sigma|}\left(P_x\vec{e}_x + P_y\vec{e}_y + P_z\vec{e}_z\right).
\end{aligned}$$

Then vector $\vec{v}$ in the new system of reference will be expressed as follows

$$\vec{v'} = \begin{pmatrix} \frac{P_z}{\sqrt{P_x^2+P_z^2}} & 0 & \frac{-P_x}{\sqrt{P_x^2+P_z^2}} \\ \frac{-P_xP_y}{|\vec{P}_\Sigma|\sqrt{P_x^2+P_z^2}} & \frac{P_x^2+P_z^2}{|\vec{P}_\Sigma|\sqrt{P_x^2+P_z^2}} & \frac{-P_yP_z}{|\vec{P}_\Sigma|\sqrt{P_x^2+P_z^2}} \\ \frac{P_x}{|\vec{P}_\Sigma|} & \frac{P_y}{|\vec{P}_\Sigma|} & \frac{P_z}{|\vec{P}_\Sigma|} \end{pmatrix} \vec{v}. \tag{16}$$

After the rotation $\vec{p'_+} = \{p'_x, p'_y, p'_{+z}\}$ and $\vec{p'_-} = \{-p'_x, -p'_y, p'_{-z}\}$;

$$\vec{\beta}_{\text{cms}} = \frac{\vec{P}'_\Sigma}{E_\Sigma} = \frac{\{0, 0, p'_{+z} + p'_{-z}\}}{E_+ + E_-}; \tag{17}$$

$$Q^*_L = \gamma\left((p'_{+z} - p'_{-z}) - \beta_{\text{cms}}(E_+ - E_-)\right) = 2\frac{p'_{+z}E_- - p'_{-z}E_+}{\sqrt{(E_+ + E_-)^2 - (p'_{+z} + p'_{-z})^2}}. \tag{18}$$

Finally

$$Q^*_x = 2p'_x, \qquad Q^*_y = 2p'_y, \qquad Q^*_L = \frac{2}{M}\left(p'_{+z}E_- - p'_{-z}E_+\right), \tag{19}$$

here M — pairs effective mass.

[3]The secondary horizontal system is the target system of reference rotated by 100 mrad around its x-axis.

References

[1] A. Lanaro, *Parameterisation of correlated and accidental particle spectra*, DIRAC internal note 2001-01.

[2] C. Santamarina, *DIRAC event generator*, DIRAC internal note, 2004-02.

[3] M. Zhabitsky, *Parametrization of single particle spectra at the DIRAC kinematic range*, DIRAC internal note, 2006-06.

[4] L. Afanasev, M. Gallas, V. Karpukhin, A. Kulikov, *First level trigger of the DIRAC experiment*, Nucl. Instr. Meth. A479 (2002) 407.

[5] L. Afanasyev et al., *The multilevel trigger system of the DIRAC experiment*, Nucl. Instr. Meth. A491 (2002) 376.

[6] P. Kokkas, M. Steinacher, L. Tauscher, S. Vlachos, *The neural network first level trigger for the DIRAC experiment*, Nucl. Instr. Meth. A471 (2001) 358.

[7] A. Benelli, L. Tauscher, *RNA trigger simulation*, DIRAC internal note, 2006-01.

[8] V. Yazkov, *private communication*.

[9] *Criteria for pre-selection*, http://www.cern.ch/DIRAC/pre-sel.html

[10] V. Brekhovskikh, *The analysis of data adequacy for Ni 2001*, DIRAC internal note, 2003-07.

[11] G.D. Badhwar, S.A. Stephens, and R.L. Golden, *Analytic representation of the proton-proton and proton-nucleus cross-sections and its application to the sea-level spectrum and charge ratio of muons*, Phys.Rev. **B15** (1977) 820.

[12] D. Drijard, M. Hansroul, V. Yazkov, *DIRAC offline reconstruction program Ariane*, http://www.cern.ch/dirac.

[13] P. Zrelov, V. Yazkov, O. Gortchakov, *The GEANT-DIRAC simulation program*, http://www.cern.ch/dirac.